International Journal of Research in Advent Technology, Vol.6, No.7, July 2018
E-ISSN: 2321-9637
Available online at www.ijrat.org

Effect of heat input on the characteristics of 304L austenitic stainless steel weld deposited by GTAW for root pass and SMAW for filler passes

Harsimranjit Singh Randhawa[1], Sunil Kumar[2]
*#Student M.Tech. (Mechanical Engg.), *Assistant Professor (Mechanical Engg.) [Supervisor]*
Yadavindra College of Engineering, Punjabi University Guru Kashi Campus,
Talwandi Sabo, Bathinda, Punjab, India - 151302.
**Corresponding Author Email: sunilbaghla@yahoo.co.in*

Abstract-A 10mm thick 304L austenitic stainless steel plate has been welded using single V-joint configuration approaching the joint from a single side. Back purging has been employed to protect the rear side of the root pass weld metal against oxidation. The root pass has been deposited by gas tungsten arc welding (GTAW) process and filler passes are deposited by shielding metal arc welding (SMAW) process at 90A and 120A welding currents giving heat inputs of the order of 0.679 and 0.933 kJ/mm respectively at a constant speed of weld deposition. It has been concluded that micro-hardness of weld metal and heat affected zone (HAZ) of weldments produced at lower heat input is higher while the impact toughness value of weld metal and HAZ is lower as compared to higher heat input. All the tensile specimens produced at low as well as high heat inputs were fractured from the base material indicating that the tensile strength of weld metal is higher than the base material. In root bend test, a crack was found at the root of a specimen at lower heat input showing loss of ductility or incomplete root penetration or lack of fusion. It is recommended that weld joints are needed to be fabricated using high heat input of the order of 0.93kJ/mm produced by 120A welding current to achieve the better joint characteristics with greater toughness.
Index Terms- Austenitic stainless steel 304L, GTAW, SMAW, weld heat input, back purging, impact strength, tensile strength, toughness, micro-hardness, weldment.

1. INTRODUCTION

Austenitic stainless steel is a family of iron-chromium-nickel alloys with a low level of carbon. The austenitic stainless steel 304L is easiest to weld giving a high degree of toughness even in the as-welded condition [1]. The weldability of austenitic stainless steel is governed by their susceptibility to hot cracking. Excessive heat input may result in weld cracking, loss of corrosion resistant, warping and undesirable changes in mechanical properties. This alloy can be used in the "as welded condition" even in severe corrosive conditions [2]. Stainless steel welds generally require 20- 30% less heat input than welds in carbon steels due to lower thermal conductivity and higher electrical resistance of stainless steels [3]. Because of the low thermal conductivity more heat is available to melt the material producing detrimental results. Excessive heat gives large thermal gradients across the joint resulting distortion. Heat input can be reduced by using low welding current, low arc voltage, higher travel speed & stringer beads [3].

2. RELATED RESEARCH WORK

Choubey and Jatti (2014) [4] explained the effect of heat input by welding current, arc voltage and welding speed on mechanical properties and microstructure of austenitic 202 type stainless steel weldments produced by SMAW. Authors concluded that with the increase in heat input, tensile strength decreases and fractured surfaces shows the ductile and brittle failure of the part sample. Experimental results state that the micro hardness of joint increases with the increase of heat input. **David et al. (1995) [5]** explained the method to prevent hot cracking by a small percentage of austenitic stainless steel. Due to exposure to high temperatures for a long time, a continuous network of carbide forms at the austenite/ferrite interface that reduces the elevated temperature properties of austenitic stainless steel welds. **Kumar and Shahi (2011) [6]** showed the effect of heat input on the microstructure and mechanical properties of 304 austenitic stainless steel joint using GTAW. Highest tensile strength was reported for the joint made at lowest heat input. Grain coarsening of HAZ was reported at all the heat inputs but it increases with the increase of heat input. The tensile properties of the joint are dependent on the microstructure developed at different heat inputs. **Mukesh and Sharma (2013) [7]** reported the effect of weld heat input on the mechanical properties of 6 mm thick square-butt weld joint of type 202 austenitic stainless steel produced by GTAW and L9 orthogonal array of Taguchi's methodology was applied. Welding current was found to be a most significant parameter that influenced the tensile strength and micro hardness. **Nnuka et al. (2015) [8]** reported the effect of the welding current and filler metal on the percentage elongation of GTAW austenitic stainless steel weld joint. A higher percentage of elongation was reported by using higher welding current attributed to the poor thermal conductivity of base material that resulted in grain growth with its softening effect. It is concluded that percentage elongation is lower for all currents and filler metals than that of base materials. **Singh et al. (2013) [9]** investigated the mechanical properties of the multi-pass weld joint of 304 stainless steel using shielded metal arc welding process. It was revealed that the weld joint deposited using low heat input possessed better tensile strength. The micro hardness of heat affected zone (HAZ) of weld deposited by using low heat input was found higher than that of weld deposited by taking high heat input combinations. **Tabish et al. (2014) [10]** studied the effect of heat input on the microstructure and mechanical properties of a GTA welded joint. The highest tensile strength was found with the weld joint produced by using low heat input. Micro-hardness of the upper surface of the weld was greater than the weld center. **Vinoth et al. (2015) [11]** investigated the comparison of mechanical properties of 304L austenitic stainless steel weld joint produced by SMAW, GMAW and GTAW processes. Experimental results showed that yield strength, ultimate tensile strength and toughness were superior with the joints produced by GTAW in comparison to SMAW due to more weld penetration at the given weld deposition parameters. **Yan et al. (2010) [12]** have investigated the microstructure and mechanical properties of 304 stainless steel joints by GTAW, laser welding, and laser-GTAW hybrid welding. The result revealed that the joint by laser welding has the highest tensile strength and smallest dendrite size in all joints while the joint by GTAW has the lowest tensile strength and biggest dendrite size.

3. RESEARCH GAPS AND PROBLEM FORMULATION

After studying the literature and key research papers, it has been found that little work has been reported related to deposition of the stainless steel weld with single V-joint configuration and approaching the joint from one side. The single V-joint configuration necessitates the use of back purging arrangement as the joints welded without purging also require grousing, grinding or picking to remove the oxidize weld metal to regain resistance to corrosion. The present work is motivated by the fact that the study of the welding of stainless steel approaching the joint from one side with back purging will be of great help. This work will definitely be helpful to find out the strengths, weaknesses and other important factors related to process and the joint. It has also been observed that heat input to the weld can be varied by changing the welding current, arc voltage and speed of weld deposition. There is an optimum heat input for a given plate thickness, joint configuration, and type of stainless steel being welded to achieve desired joint characteristics.

4. EXPERIMENTATION

4.1. *Samples*

A 10mm thick austenitic stainless steel plate grade AISI 304L plates were butt welded selecting a single V-groove joint configuration with 65^0 groove angle as shown in fig. 1.

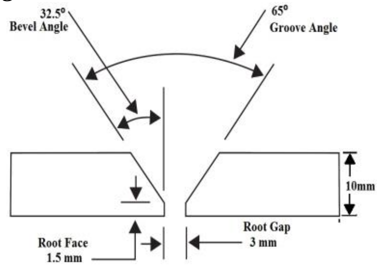

Fig. 1: V-groove butt weld joint [17]

The root weld pass was deposited using 1.2 mm diameter austenitic stainless steel type 308L filler wire. The rest filler passes were deposited using 3.15 mm diameter type 308L-16 Rutile electrodes. The chemical composition of the base material, filler wire and electrode are also detailed in table 1.

Table 1: Composition of base and filler material [1]

Material		Base material 304L	Wire 308L	Electrode 308L-16 Rutile
Chemical Composition (wt. %)	Cr	18.17	20.00	19.80
	Ni	8.08	9.00	10.00
	C	0.010	0.020	0.030
	Mn	1.56	2.00	1.40
	Si	0.35	0.40	0.40
	P	0.025	0.020	-
	S	0.010	0.015	-

An Inverter type power source USHA TIG 315P with constant current characteristic and a water-cooled welding torch was used for GTAW welding of samples. The technical specification of the power source is Input: 3ϕ 400V, Welding current GTAW: 10-315(A), Welding current SMAW: 10-295(A), Duty cycle: 60%, Arc ignition: High frequency, No load voltage: 45V, Gas pre-flow: 0-2 (l/s), Gas post flow: 0-10 (l/s). Fig. 2 (a & b) shows the specimens confirming to relevant ASTM standard.

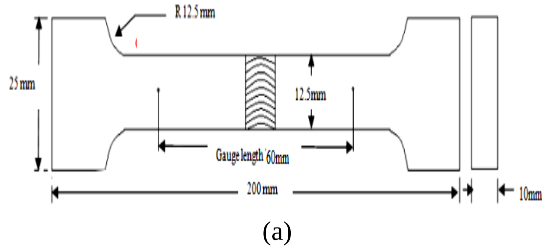

(a)

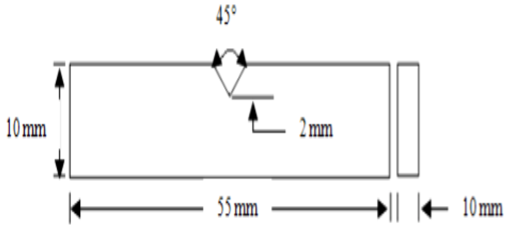

(b)
Figure 2: Samples as per ASTM standards [1, 2, 3]

4.2 Back Purging Fixture

Fig. 3 shows the fixture for back purging. It was constructed out of $460mm \times 260mm \times 30mm$ thick mild steel plate by machining $25mm \times 10mm$ recess in the center of steel plate as shown in fig. 2 to fix $25mm \times 10mm$ thick grooved copper plate. The holes of 1.5mm diameter with counter shank of 3mm diameter were drilled at the center of grooved copper plate for purging of argon gas to protect the underside of root pass. Two ports for argon gas inlet and outlet with pressure control knob were provided. The plates are to be welded are placed 3mm apart so that uniform fusion of root edges takes place during the welding process.

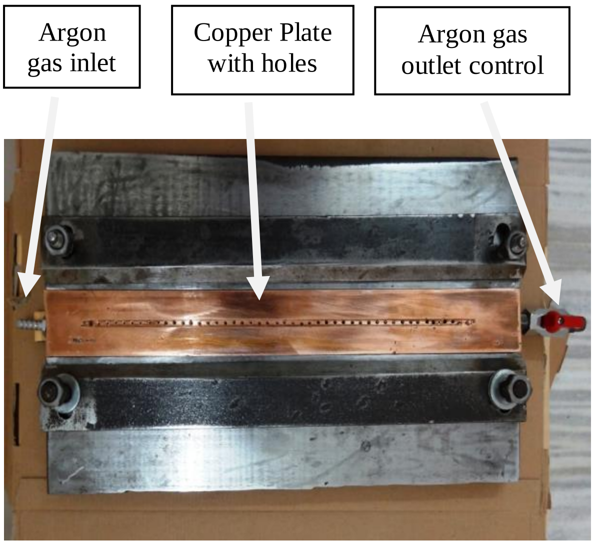

Fig. 3: Fixture to hold the plates along with back purging arrangement

4.3 Weld Deposition

The root pass was deposited by GTAW process using direct current electrode negative (DCEN) [straight polarity] for narrow and deep penetration. The root pass was deposited at 95A welding current and 9V arc voltage with an average weld heat input of 2.13 kJ/mm. The welds were deposited at 90A (for low heat input) and 120A (for high heat input) to explain the influence of heat input on the mechanical properties of the joint. Table 2 and 3 shows welding parameters at welding current 90A and 120A respectively. The average heat input for GTAW was resulted in 2.13 kJ/mm and for SMAW was 0.933 kJ/mm.

Table 2: Welding parameters at 90A welding current

Weld Layers	1	2	3	4	5
Passes	Root	Filler	Filler	Filler	Cap
Weld Process	GTAW	SMAW	SMAW	SMAW	SMAW
Electrode/ Wire Size (mm)	1.6	3.14	3.14	3.14	3.14
Current (A)	95	90	90	90	90
Voltage (V)	9	23	23	23	23
Polarity	DCEN	DCEP	DCEP	DCEP	DCEP
Deposition speed mm/sec (S)	0.4	3.0	2.8	3.2	3.1
Heat Input kJ/mm $\frac{A \times V}{S \times 1000}$	2.130	0.690	0.771	0.618	0.638
Average Heat Input kJ/mm	2.130	0.679			

Table 3: Welding parameters at 120A Welding current

Weld Layers	1	2	3	4
Passes	Root	Filler	Filler	Cap
Weld Process	GTAW	SMAW	SMAW	SMAW
Electrode/ Wire Size (mm)	1.6	3.15	3.15	3.15
Current (A)	95	120	120	120
Voltage (V)	9	21	22	21
Polarity	DCEP	DCEN	DCEN	DCEN
Deposition speed mm/sec (S)	0.4	2.8	3.1	2.4
Heat Input kJ/mm $\frac{A \times V}{S \times 1000}$	2.13	0.9	0.85	1.05
Average Heat Input kJ/mm	2.130	0.933		

5. RESULTS AND DISCUSSIONS

5.1 The surface of weld deposit

The surface appearance of the top and root reinforcement of the weld deposited at 90 A and 120 A welding current is shown in fig. 4 (a-d).

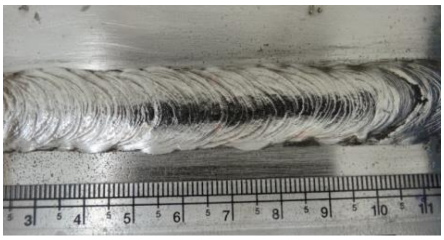

(a) *Top bead at 90A*

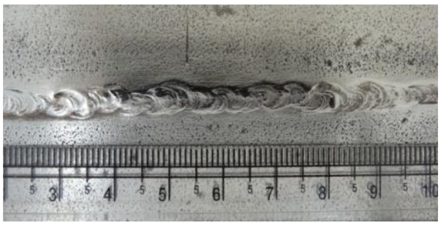

(b) *Root at 90A*

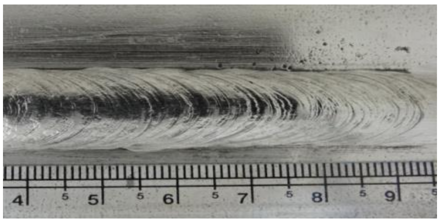

(c) *Top bead at 120A*

(d) *Root at 120A*

Fig. 4 (a-d): Appearance of top bead and Root reinforcement at different welding currents

Fig. 4 (a) and 4(c) shows a bead of the weld deposited by SMAW at both the welding currents of 90A and 120A. Fig. 4(b) and 4(d) show penetration of the root pass deposited by GTAW. It can be seen that root reinforcement deposited at 120A is wider than deposited at 90A.

5.2 Micro Hardness Test

Table 4 lists the micro-hardness of the base material, weld metal, and heat-affected zone. The average value of micro-hardness of the base material has been found out as 227 VHN.

Table 4: Micro-hardness of base metal, weld metal, and heat affected zone

Welding current (*A*)	Heat input *(kJ/mm)*	Base material *(VHN)*	Weld material *(VHN)*	Heat affected zone *(VHN)*
90	0.68	220-234	249-250	306–314
120	0.93	220-234	220-240	235-260

The micro hardness of weld metal and heat affected zone decreases with the increase in welding current from 90A to 120 A as tabulated in table 4. It can be ascribed to cooling rate that decreases with the increase of heat input at higher welding current and the micro-hardness is directly related to the cooling rate at that point. The higher cooling rate will produce higher micro-hardness. At a given welding current the micro hardness of heat-affected zone has been found higher than that of weld metal. The heat affected zone adjoining to base material experiences relatively higher cooling than weld metal resulting higher hardness than weld metal.

5.3 Tensile Strength Test

In the tensile test, all the specimens of 90A and 120A welding current were fractured from the base material revealed that the strength of weld metal is over matching than that of base material i.e. higher tensile strength than base material as shown in fig. 5.

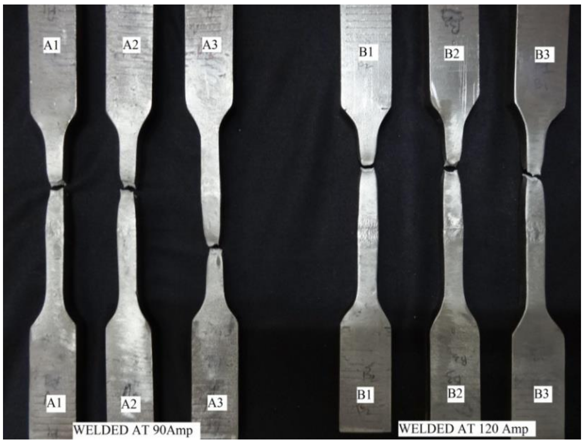

Fig. 5: Fracture location in base material at 90A and 120A welding current

5.4 Impact Toughness Test

The Charpy V - notch toughness of weld metal and heat affected zone (HAZ) produced at 90A and 120A welding current has been presented in table 5. It is concluded that for 90A welding current, the average toughness of weld metal and HAZ is 161J and 241J respectively and for 120A welding current, the average toughness of weld metal and HAZ is 194J and 270J respectively. The average value of Charpy V-notch impact toughness of base material has been found out of the order of 284J. Table 5 depicts the Charpy V- notch impact toughness of weld metal and heat affected zone increases with the increase in welding current. This is in line with the fact that the micro-hardness decreases with the increase of welding current.

Table 5: Charpy V- notch impact toughness of weld metal and HAZ produced at 90A and 120A

Type of Specimen	Sample	Notch Location	Energy absorbed in fracture of weld deposited at welding current (J)		Average Energy absorbed in fracture of weld deposited at welding current (J)	
			90 (A)	120 (A)	90 (A)	120 (A)
Weld Metal	1	Perpendicular to the direction of the weld	170	202	161	194
	2		168	182		
	3		145	198		
HAZ	1	1mm from the fusion line	220	261	241	270
	2		246	267		
	3		256	281		

The impact test specimen for weld metal and heat affected zone after the test are shown in fig. 6.

(a)

(b)

Fig. 6: Charpy V- Notch tested specimens at 90A and 120A welding currents

The Charpy V- notch impact toughness of the base material, weld metal and heat affected zone has been presented in the bar chart in fig. 7. The bar chart depicts that toughness of weld metal and the heat affected zone is significantly higher in weldments produced at 120A welding current than that of producing at 90 A welding current.

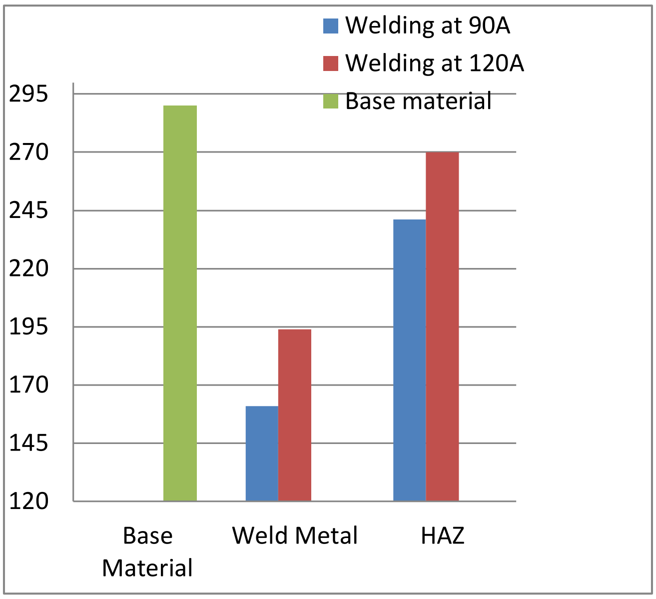

Fig. 7: Comparison of impact values of the base material, HAZ and weld metal

5.5 *Bend Test*

The root bend test was conducted on the specimens machined out from the weldments deposited at 90A and 120A welding currents. Higher ductility has been found with the specimens produced at 120A welding current giving higher heat input of the order of 0.93 kJ/mm and no crack was visible after bending when the root of the joint was subjected to tension.

A crack at root was observed in one of the bent test specimens of 90A welding current giving heat input of the order of 0.68kJ/mm. This can be attributed to a loss in ductility or incomplete root penetration /lack of fusion as shown in fig. 8.

Fig. 8: Root bend test specimens at 90A and 120A

6. CONCLUSIONS AND FUTURE SCOPE

Complete root penetration with back purging was successfully achieved with appropriate root reinforcement. In root bend test all the specimens of 120A welding current were successfully bent without showing any crack at the root side which was subjected to tension. The micro-hardness of weld metal and heat affected zone of weldments produced at lower heat input (90A welding current) is higher and impact toughness valve is lower than that of weldments produced at a higher heat input (120A welding current). The higher toughness of weld metal and HAZ resulted in joints produced at 120A welding current. Hence, it is recommended to deposit the weld at 120A welding current to achieve better joint characteristics with enhanced toughness and higher productivity. Weld can be deposited selecting higher welding currents in the range of 100A to 160A welding current using 3.15 and 4.00 mm diameter shielded metal covered electrodes type ASW E308L Rutile. Work can be extended to inter-crystalline corrosion test. Authors are working in this direction currently.

REFERENCES

[1] American Society for Testing and Materials ASTM E8-15, “Standard Test Methods for Tension Testing of Metallic Materials”.

[2] American Society for Testing and Materials ASTM E23-12, “Standard Test Methods for Notched Bar Impact Testing of Metallic Materials”.

[3] American Society for Testing and Materials ASTM E290-14, “Standard Test Methods for Bend Testing of Material for Ductility”.

[4] Choubey A.; Jatti V.S. (2014): Influence of heat input on mechanical properties and microstructure of austenitic 202-grade stainless steel weldments, World Scientific and Engineering Academy and Society, **9**, pp. 222-228.

[5] David S.A.; Vitek J.M.; Alexander D.J. (1995): Embrittlement of austenitic stainless steel welds, Scientific and Technical Information, **5**, pp. 1-8.

[6] Kumar S.; Shahi A.S. (2011): Effect of heat input on the microstructure and mechanical properties of gas tungsten arc welded AISI 304 stainless steel joints, Materials & Design, **32**, pp. 3617-3623.

[7] Mukesh; Sharma S. (2013): Study of mechanical properties in austenitic stainless steel using gas tungsten arc welding (GTAW), International Journal of Engineering Research, **3**, pp. 547-553.

[8] Nnuka E.E.; Okonji P.O.; Nwoye C.I.; Akaluzia R.O. (2015): Effect of welding current and filler metal types on percent elongation of GTAW austenitic stainless steel welds joints, Electronic Journal Management System, **2**, pp. 1-5.

[9] Singh T.; Shahi A.S.; Kaur M. (2013): Experimental studies on the effect of multipass welding on the mechanical properties AISI 304 stainless steel SMAW joints, International Journal of Scientific and Engineering Research, **4**, pp. 951-961.

[10] Tabish T.A.; Abbas T.; Farhan M.; Atiq S.; Butt T.Z. (2014): Effect of heat input on microstructure and mechanical properties of the TIG welded joints of AISI 304 stainless steel, International Journal of Scientific and Engineering Research, **5**, pp. 1532-1541.

[11] Vinoth V.; Madhavan R.; Tharanitharan G. (2015): Investigation on property relationship in various austenitic stainless steel 304L welds, International Journal of Scientific and Research Publications, **5**, pp. 1-4.

[12] Yan J.; Gao M.; Zeng X. (2010): Study of microstructure and mechanical properties of 304 stainless steel joints by TIG, laser and laser TIG hybrid welding, Optics and Lasers in Engineering, **48**, pp. 512-517.